NEOPLASIA
www.neoplasia.com

Volume 12 Number 4 April 2010 pp. 294–304 294

The Extracellular Matrix Glycoprotein Elastin Microfibril Interface Located Protein 2: A Dual Role in the Tumor Microenvironment[1,2]

Maurizio Mongiat[*,3], Stefano Marastoni[*,3], Giovanni Ligresti[*,4], Erica Lorenzon[*], Monica Schiappacassi[*], Roberto Perris[*,†], Sergio Frustaci[‡] and Alfonso Colombatti[*,§]

*Experimental Oncology Division 2, CRO-IRCCS, Aviano, Italy; [†]University of Parma, Parma, Italy; [‡]Division of Medical Oncology, CRO-IRCCS, Aviano, Italy; [§]MATI Center of Excellence University of Udine, Udine, Italy

Abstract

We have recently reported that elastin microfibril interface located protein 2 (EMILIN2), an extracellular matrix (ECM) glycoprotein, triggers cell death through a direct binding to death receptors. EMILIN2 thus influences cell viability through a mechanism that is unique for an ECM molecule. In the present work, we report an additional function for this molecule. First, we identify the region responsible for the proapoptotic effects, a 90-amino acid residue-long coiled-coil fragment toward the N-terminus of the molecule. The fragment recapitulates EMILIN2 proapoptotic mechanisms. In addition, using either the full molecule or the active fragment, for the first time, we demonstrate a significant antitumoral effect *in vivo*, likely due to a decrease in tumor cell viability. Unexpectedly, tumors treated with EMILIN2 or the deletion mutant display a significant increase of tumor angiogenesis. In view of this novel finding, the cotreatment of the growing tumors with an antiangiogenic drug led, in most cases, to a complete regression of tumor growth. These results grant further support to recent findings that pinpoint the microenvironment as an important regulator of cell fate under both physiological and pathological conditions and disclose the possibility of using EMILIN2 fragments as potent antineoplastic tools for cancer treatment.

Neoplasia (2010) 12, 294–304

Introduction

Tumor growth is profoundly influenced by the neighboring cells and microenvironment [1,2]. In this scenario, tumors represent functional tissues interconnected with a large variety of cell types, blood and lymphatic vessels, embedded in a complex network of extracellular matrix (ECM) molecules composing the microenvironment, which are thought to sustain tumor cell survival, growth, and dissemination to distant organs [3]. For this reason, in the recent years, researchers have focused the attention on ECM and cell components of the microenvironment as potential targets or tools for anticancer therapy. Endothelial cells (ECs), for instance, are promising targets because, unlike tumor cells, they are genomically stable and thus less prone to drug resistance. Judah Folkman [4] first foresaw the possibility to target blood vessels instead of the tumor itself with the aim of halting the nutrients and oxygen supply to the aberrantly proliferating cells. These efforts have led to the discovery of many antiangiogenetic molecules such as bevacizumab, an anti–vascular endothelial growth factor (VEGF) antibody currently used in clinics in combination with conventional chemotherapy for different types of tumors [5–9]. In addition, tumor growth depends on the cell's capability to proliferate and survive despite apoptotic stimuli. Resistance to apoptosis is indeed one of the hallmarks of cancer and is achieved through the inactivation of the finely regulated mechanisms that control this process [10,11]. Apoptosis is achieved through the initiator caspases of the so-called intrinsic and extrinsic apoptotic pathways

Abbreviations: DISC, death-inducing signaling complex; EC, endothelial cell; ECM, extracellular matrix; HUVEC, human umbilical vein endothelial cell; MTT, 3-(4,5-dimethylthiazol-2-yl)-2,5 diphenyltetrazolium bromide; TUNEL, terminal deoxynucleotide transferase dUTP nick end labeling

Address all correspondence to: Maurizio Mongiat, PhD, Department of Molecular Oncology and Translational Research, CRO-IRCCS, via Franco Gallini, 2 Aviano (PN), Italy. E-mail: mmongiat@cro.it

[1]The authors thank the ISS-ACC Program 2, the Associazione Italiana per la Ricerca sul Cancro and MIUR Fondi di Investimento per la Ricerca di Base (grant no. RBRN07BMCT) for supporting this work. No potential conflicts of interest are disclosed.

[2]This article refers to supplementary materials, which are designated by Figures W1 and W2 and are available online at www.neoplasia.com.

[3]These two authors contributed equally to this work.

[4]Current address: Department of Pathology, University of Washington, Seattle, WA 98195.

Received 17 November 2009; Revised 26 January 2010; Accepted 27 January 2010

DOI 10.1593/neo.91930

[12]. The extrinsic pathway is triggered through the engagement of specific receptors such as DR4 (TRAIL-R1) [13] and DR5 (TRAIL-R2) [14] by their respective death ligands [12,15]. Among these ligands, the tumor necrosis factor–related apoptosis-inducing ligand (TRAIL) is a promising cancer therapeutic tool owing to its selective action on neoplastic cells [16–18]. TRAIL binds to its receptors as a homotrimer-inducing death receptor clustering in lipid rafts followed by death-inducing signaling complex (DISC) assembly and caspase-8 [19] and caspase-10 activation [20].

Conversely, tumor cells receive prosurvival cues from different constituents of the ECM through integrin receptors through which they sense their three-dimensional location [21]. In contrast, other ECM molecules impair cell viability. Among these proteins, CCN1 can either induce or suppress apoptosis through the integrin $\alpha_6\beta_1$ and syndecan-4 [22,23]. Thrombospondin-1 stimulates apoptosis through the CD36/p59fyn pathway [24]. Endostatin halts ECs' viability through the suppression of apoptosis inhibitors such as Bcl-2 or through autophagy [25,26]. The secreted protein acidic and rich in cysteine (SPARC) functions as a tumor suppressor in various cancers [27] and induces caspase-8 activation in a death receptor–independent manner [28], whereas decorin induces caspase-3 activation [29]. Elastin microfibril interface located protein 2 (EMILIN2), a member of the EMILIN family, is characterized by the cysteine-rich EMI domain at the N-terminus, the hallmark of the family [30], α-helical domains with high probability for coiled-coil structure formation and, at the C-terminus, a proline-rich motif adjacent to a collagenous stalk preceding the globular gC1q domain [31]. Recently, we have demonstrated that EMILIN2, unique among the other ECM molecules, binds to TRAIL receptors, leading to apoptotic cell death [32].

In this study, we discover an additional property of EMILIN2; first, we identify the region responsible for the proapoptotic effects and demonstrate that, as well as the whole molecule, it exerts a potent antineoplastic action *in vivo*. Second, we found out that EMILIN2 positively affects tumor angiogenesis by acting on EC's behavior and obtained a total regression of tumor growth in combination with the anti-VEGF antibody bevacizumab. Given that neither EMILIN2 nor bevacizumab is toxic for normal cells, these results open the possibility to develop novel anticancer tools with putatively limited adverse effects.

Materials and Methods

Cell Cultures

HT1080 and HeLa cell lines were from American Type Culture Collection (ATCC, Manassas, VA) and cultured in Dulbecco's modified Eagle medium containing 10% FBS (GIBCO BRL, Milan, Italy). NHDF-Ad-Adult human dermal fibroblasts and human umbilical vein endothelial cells (HUVECs) were from Lonza S.r.l. (Milan, Italy) and were cultured in fibroblast growth medium or endothelial growth medium, respectively; embryonic kidney cells (293-EBNA cells) were a gift from Rupert Timpl (Max Planck, Munich, Germany) and were cultured in Dulbecco's modified Eagle medium containing 10% FBS and 250 μg/ml of G418 and 0.5 μg/ml of puromycin after transfection. All cells were maintained at 37°C in a humidified 5% CO_2 atmosphere.

Antibodies and Other Reagents

The 828B3B3 anti-EMILIN2 was obtained as previously described [32]. The anti-Δ4 polyclonal antibody was obtained after the injection of 150 μg of the recombinant fragment in rabbit (three total boosters). The anti–cleaved Poly(ADP-ribose) polymerase polyclonal antibody, anti-FADD antibody, FLICE/caspase 8 fluorimetric Protease Assay Kit, and ApopTag Apoptosis Detection Kit were from Chemicon International (Temecula, CA). Anti–caspase 3 and anti–type I collagen antibodies were from Santa Cruz Biotechnology, Inc., Santa Cruz, CA. The anti-DR4, anti–β-actin, anti-FLAG antibodies, the FLAG peptide, the anti-FLAG M2 affinity gel, and the human fibronectin were from Sigma-Aldrich S.r.l. (Milan, Italy) and Alexis (Plymouth Meeting, PA). The secondary HRP-conjugated antibodies were from Amersham (GE Healthcare S.r.l., Milan, Italy). The secondary antibody conjugated with Alexa Fluor 680 was from Invitrogen S.r.l. (Milan, Italy). The anti–histidine monoclonal antibody was from Abgent (Resnova S.r.l., Rome, Italy). The anti–glutathione *S*-transferase (GST) monoclonal antibody was from Abcam (Cambridge, MA). The Ni-NTA agarose was from QIAGEN (Milan, Italy). The Cell Death Detection ELISA^{PLUS} Kit (used exclusively for the experiment in Figure 3*F*) and *In Situ* Cell Death Detection Fluorescein Kit were purchased from Roche Diagnostics S.p.A. (Milan, Italy). BD Adeno-X Rapid Titer Kit was from BD (Buccinasco, Milan, Italy). Caspase-Glo 8 and Caspase-Glo 3/7 assays were from Promega S.r.l. (Milan, Italy) and were used on tumor lysates according to the manufacturer's instructions.

DNA Constructs

EMILIN2 deletion constructs Δ1 and Δ2 were generated using the *Eco*NI and *Nar*I restriction enzymes and the available pcDNA3.1-EMILIN2 construct [32]. Δ3 and Δ4 complementary DNA were amplified with the following oligonucleotides: forward 5′-CTAGCTAGCAGACACCACTGTTAGTGGA-3′ and reverse 5′-CGGGATCCTTATTCTTCA GCGTTCTTCTC-3′; forward 5′-CTAGCTAGCAGGCCCGCAGCCCGGGTAT-3′ and reverse 5′-CGGGATCCTTAAGGCTTGGGGTGCTGGCT-3′. EMILIN2 and Δ4 were subcloned in pDNR-CMV plasmid by the *Sal*I and *Bam*HI restriction enzymes. The following oligonucleotides were used: forward 5′-CCCAAGCTTGTCGACCCACATGAGGGCCTGG ATCTTCTT-3′ and the above two reverse oligonucleotides. Wild-type DR4 (wtDR4), truncated DR4 mutant (tDR4), and TRAIL were reverse-transcribed from total RNA extracted from the HeLa cell line and cloned into pcDNA3.1/Myc-His. The following oligonucleotides were used: forward 5′-CCCAAGCTTATGGCGCCACCACCAGCT-3′ and reverse 5′-TGGATATCTCTCCAAGGACACGGCAGAGC-3′; the reverse oligonucleotide for the tDR4 was as 5′-GCTCTAGAGAGACCCAAGCGCCAGAA-3′. The forward oligonucleotide for TRAIL containing a FLAG tag was 5′-CTAGCTAGCCGACTACAAGGACGACGATGACAAGACCTCTGAGGAAACCATTTC-3′ and the reverse was 5′-CGTGAGCGGCCGCCAGGTCAGTTAGCCAACT-3′. The fragment was cloned into the pCEP-Pu vector and expressed in 293-EBNA cells. The extracellular regions of DR4 were cloned into the pGEX-KG vector with the following oligonucleotides: forward 5′-CGGGATCCGCGAGTGGGACAGAGGCA-3′ and reverse 5′-GGAATT CATTATGTCCATTGCCTGA-3′.

Cell Transfection, Expression, and Purification of Recombinant Proteins

Expression of the recombinant molecules was carried out after transfection of 293-EBNA cells as previously described [32]. Proteins were purified by means of the Ni-NTA or anti-FLAG beads. HT1080 cell

lines were transfected using FuGene6 reagent (Roche Diagnostics S.p.A., Milan, Italy) according to the manufacturer's instructions.

Adenoviral Transduction

The pDNR-CMV constructs were transferred into the Adeno-X-TRE acceptor vector through Cre-loxP recombination. The recombination products have been analyzed by polymerase chain reaction and enzyme restriction. Adenovirus was produced by transfecting HEK 293 cells, and the virus titration was determined using the Adeno-X Rapid Titer Kit (Clontech, EuroClone S.p.a., Milan, Italy). HT1080 cells were cotransduced with a regulatory virus (Adeno-X Tet-On; Clontech) and the response of EMILIN2- and Δ4-recombinant viruses using 2 μg/ml of doxycyline for induction.

Western Blot Analysis

Proteins were resolved in 4% to 20% Criterion Precast Gels (Bio-Rad Laboratories, Milan, Italy) and transferred onto Hybond-ECL nitrocellulose membranes (Amersham, GE Healthcare). Membranes were blocked with 5% dry milk in Tris-buffered saline Tween-20, probed with the appropriate antibodies, and the blots were developed using Enhanced chemiluminescence (Amersham Biosciences, Cologno Monzese, Italy). Alternatively, the Odyssey Infrared Imaging System was used (Li-COR Biosciences, Lincoln, NE).

Analysis of DISC Assembly and GST Pull-down Assay

Immunoprecipitation of the DISC complex was carried out as previously described [32]; an equimolar amount (37.5 nM) of EMILIN2, Δ4, TRAIL, or type I collagen was used, and the cells were incubated for 30 minutes at 37°C. To prevent interference with the antibodies used for immunoprecipitation, the Trueblot secondary antibody (eBiosciences, San Diego, CA) was used. The GST pull-down assay was carried out as previously described [32] using *in vitro* transcribed and translated EMILIN2, the Δ1 and Δ4 and TRAIL, and 10 μg of the recombinant DR4 extracellular region fused to the GST.

3-(4,5-Dimethylthiazol-2-yl)-2,5 Diphenyltetrazolium Bromide Assays

Cells were plated in triplicates; after the different treatments, 0.3 mg/ml of 3-(4,5-dimethylthiazol-2-yl)-2,5 diphenyltetrazolium bromide (MTT) was added, and the cells were incubated for three extra hours. The formazan crystals were solubilized with DMSO, and the absorbance was detected at 620 nm.

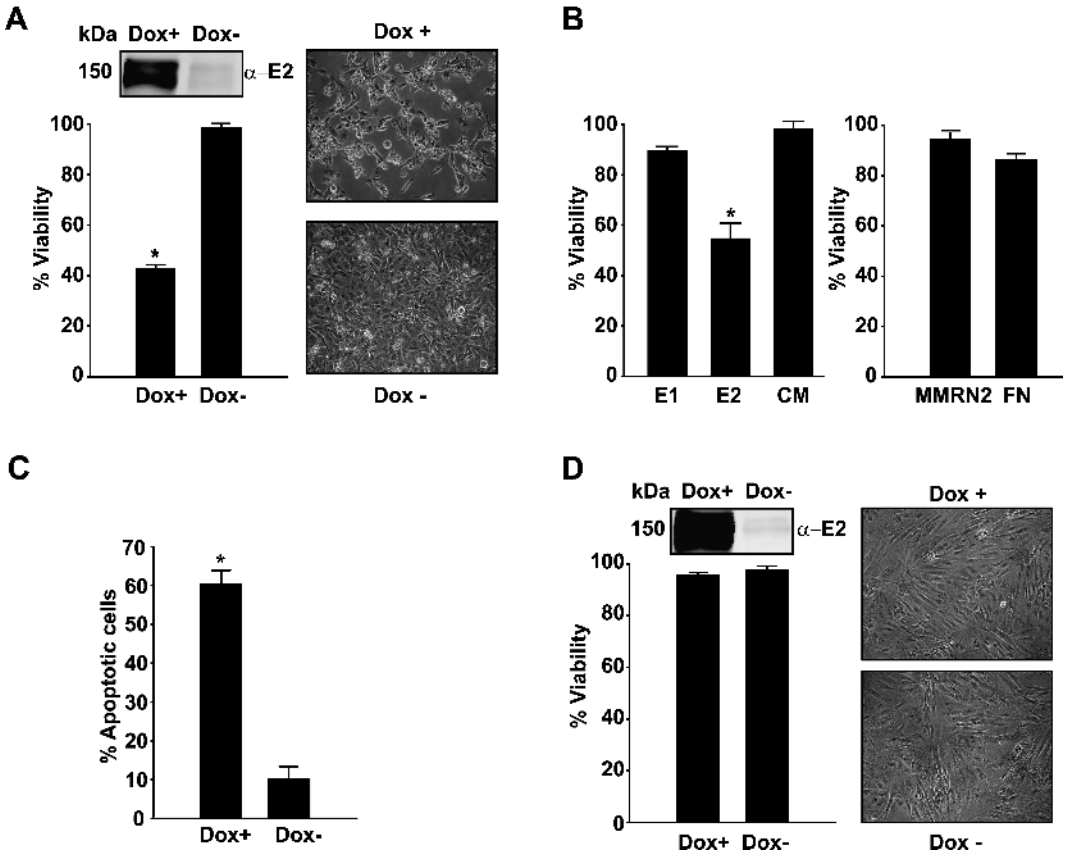

Figure 1. EMILIN2 induces apoptosis of tumor cells, leaving normal cells unharmed. (A) Top panel: Western blot analysis of EMILIN2 expression after transduction of HT1080 cells with the adenoviral construct with or without doxycycline (Dox+ and Dox−). Bottom panel: MTT assay after transduction. Right panels: Representative pictures of HT1080 cells undergoing apoptosis after overexpression of EMILIN2. Bar, 75 μm. (B) MTT assays performed on HT1080 cells after treatment with 293-EBNA conditioned media in the presence or absence of EMILIN1 or EMILIN2 (E1, E2, and CM, respectively) or with purified Multimerin2 [33] or fibronectin (MMRN2 and FN, respectively). (C) TUNEL assay performed on HT1080 cells transduced with the EMILIN2 adenoviral construct with or without doxycycline. (D) Top panel: Western blot on NHDF-Ad cells transduced with the EMILIN2 adenoviral construct with or without doxycycline. Bottom panel: Relative MTT assay. Representative pictures of the cells are on the right panels. Bar, 75 μm. *$P \leq .02$.

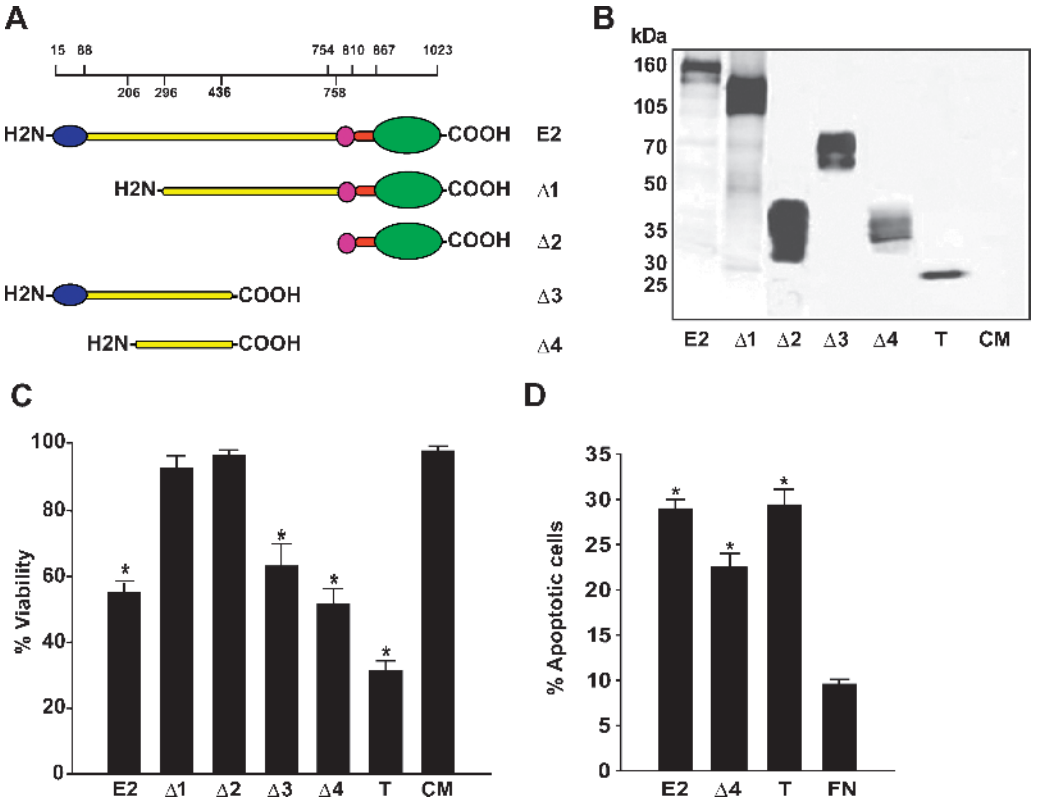

Figure 2. The EMILIN2 proapoptotic effects are recapitulated by a 90-amino acid residue region. (A) Schematic representation of EMILIN2 (E2) and the deletion mutants (Δ1 to Δ4). The position of the amino acid residues delimiting the domains is reported at the top; those corresponding to the deletions are at the bottom. *Blue* indicates EMI domain; *yellow*, coiled-coil region; *magenta*, proline-rich domain; *red*, collagenous stalk; and *light blue*, gC1q domain. (B) Western blot analysis of the conditioned media from 293-EBNA cells transfected with the EMILIN2 (E2), the various EMILIN2 deletions (Δ1 to Δ4), or TRAIL (T) constructs. An α-His antibody was used for the analysis, and conditioned medium from mock-transfected cells was used as a control (CM). (C) MTT assay performed on HT1080 cells challenged with recombinant EMILIN2 (E2), the deletion mutants (Δ1 to Δ4), or TRAIL (T). Conditioned medium (CM) from mock-transfected cells was used as control. (D) TUNEL assay performed on HT1080 cells after treatment with EMILIN2 (E2), Δ4 (Δ4), TRAIL (T), or fibronectin (FN) as a control. Data are representative of three independent experiments. $*P \leq .03$.

Terminal Deoxynucleotide Transferase dUTP Nick End Labeling Assays and Indirect Immunofluorescence

Apoptotic cells challenged with the various proteins were detected with the Cell Death Detection ELISA^{PLUS} terminal deoxynucleotide transferase dUTP nick end labeling (TUNEL) assay. For the TUNEL test on tumor sections, the specimens were embedded in OCT Embedding Matrix (Kaltek S.r.l. Padua, Italy), and 7-μm-thick cryostat sections were obtained using a MICRON cryostat (Heidelberg, Germany); apoptosis was detected with the ApopTag Peroxidase *In Situ* Oligo Ligation Apoptosis Detection Kit (Chemicon International) according to the manufacturer's instructions. Blood vessels were detected with an antimouse multimerin 2 monoclonal antibody that was produced after the injection of the purified recombinant protein in BALB/C mice [33]. Cell nuclei were stained with the TO-PRO-3 fluorescent dye (Molecular Probes, Invitrogen S.r.l.). Images were acquired with a confocal system (Leica Microsystems, Milan, Italy).

Soft Agar Colony Assay and Three-dimensional Matrigel Growth

Soft agar colony assays were carried out using 0.5% low-melting agarose as previously described [32]. HT1080 cells transduced with the Δ4 recombinant adenovirus were used in the presence or absence of 2 μg/ml doxycycline. Alternatively, equimolar amounts of recombinant fibronectin or of Δ4 (37.5 nM) were added. Pictures were obtained after 13 days of incubation, and the clones that formed by more that 10 cells were counted. The assay was performed in triplicate. For the three-dimensional Matrigel growth test, 5×10^5 HT1080 cells transduced either with the EMILIN2 or with Δ4 were embedded in 500 μl of Matrigel (BD Biosciences Euroclone S.p.a., Milan, Italy). Complete medium was added after solidification of the Matrigel drops containing the cells. After 10 days, pictures were obtained.

Colony Formation Assay

Two hundred HT1080 cells per well were plated on 12-well plates. Conditioned media from mock, EMILIN2, or Δ4 were used in the presence of 5% FBS. After 13 days, the cells were washed with PBS and stained with crystal violet; pictures were obtained and the clones were counted. Alternatively, HT1080 cells were transduced with the Δ4 adenoviral construct and were plated in the presence or absence of doxycycline.

Cell Migration Assay

Transwells with 8-μm pore membranes (BD Biosciences, Buccinasco, Italy) were coated with 10 μg/ml of denatured bovine serum albumin, type I collagen, or EMILIN2, and 150×10^3 HUVECs were used for

each point. Fifty nanograms per milliliter of VEGF (BD Biosystems) was used as a chemoattractant. After 24 hours, cells were removed from the top of the membranes, and the migrated cells on the bottom were fixed, stained with crystal violet, and counted. Each experiment was performed in triplicate and repeated three times.

Scratch Test

HUVECs cells were plated on gelatin-coated 24-well plates and, on reaching confluence, were starved for 3 hours in serum-free medium and scratched with a tip. Cells were then incubated with 10 μg/ml of EMILIN2 or type I collagen in complete diluted 1:1 with serum-free medium. Pictures were obtained over time with the Leica AF6000 Imaging System (Leica Microsystems). The percentage of cell migration was evaluated measuring the area of the scratch covered by the migrated cells by means of the Image Tool Software (http://ddsdx.uthscsa.edu/dig/itdesc.html; San Antonio, TX). Each experiment was performed in triplicate and repeated three times.

Tubulogenesis Assay

A total of 25 × 10^3 HUVECs per well were seeded on a 96-well plate on top of presolidified Matrigel (BD Biosciences Euroclone). Cells were treated with 2.5 μg/ml of purified recombinant EMILIN2 or Δ4; an equal volume of PBS was used as a control. Pictures were obtained over time with the Leica AF6000 Imaging System (Leica Microsystems). The experiment was repeated three times.

In Vivo *Tumor Growth*

Five BALB/c nude mice were subcutaneously injected with 1 × 10^6 HT1080 cells stably transfected with pcDNA3.1 vector carrying the luciferase or EGFP coding sequence. The animals were treated every 3 days with 10 μg of purified EMILIN2 or Δ3 or with an equal volume of PBS. Tumor growth was evaluated over time either using the *in vivo* Imaging System (Caliper Life Sciences S.A., France) or measuring the growing tumors with a caliper; in this case, tumor volumes were calculated using the following formula: $\pi LW^2/6$, where L indicates length and W indicates width.

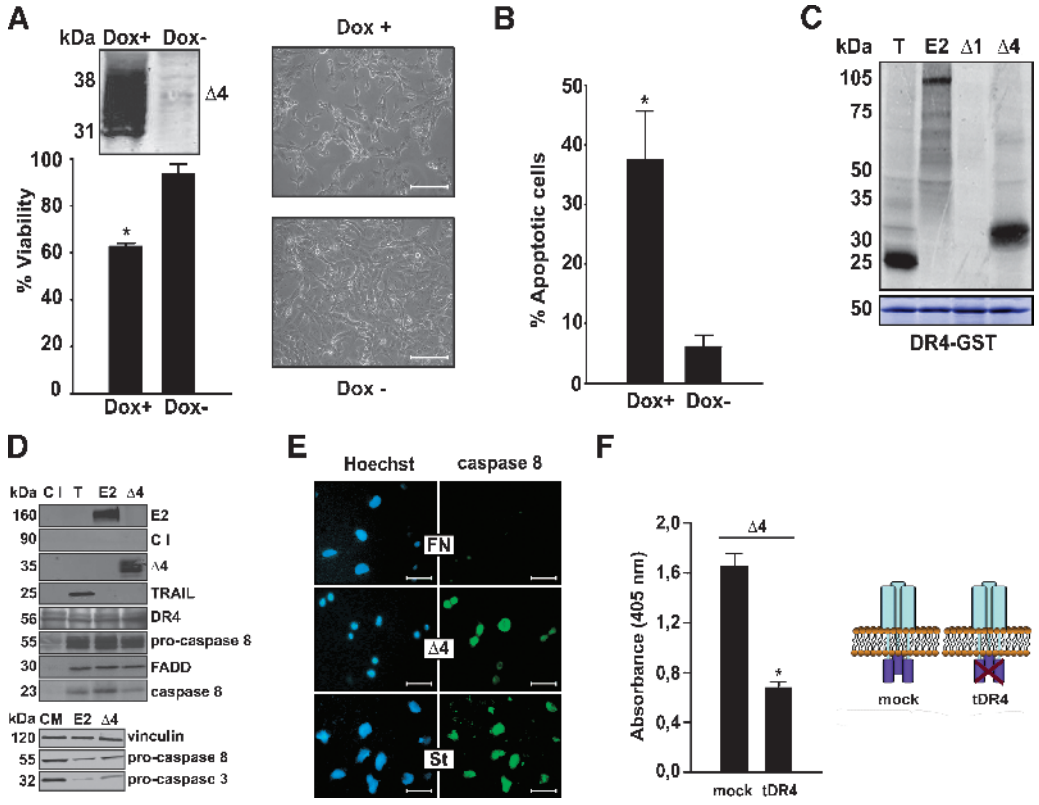

Figure 3. Δ4 induces tumor cell apoptosis through direct binding to death receptor DR4. (A) Top left panel: Western blot analysis of conditioned media from HT1080 cells transduced with the Δ4 adenoviral vector with or without doxycycline (Dox+ and Dox−, respectively). Bottom left graph: MTT assay performed on HT1080 cells. Right panels: Representative image. Bar, 75 μm. (B) TUNEL assay performed on Δ4-transduced HT1080 cells with or without doxycycline (Dox+ and Dox−, respectively). (C) GST pull-down experiment using the DR4 extracellular region fused to the GST protein incubated with TRAIL, EMILIN2, or the Δ1 and Δ4 deletion mutants (T, E2, Δ1, and Δ4, respectively). (D) Top panel: DISC immunoprecipitation after incubating HeLa cells with type I collagen, TRAIL, EMILIN2, or Δ4 (C I, T, E2, and Δ4, respectively). Immunoprecipitates were analyzed with the α-type I collagen, the α-DR4, the α-caspase-8, and the α-FADD antibodies or with α-FLAG antibody to detect EMILIN2, Δ4, or TRAIL, as indicated on the right side of the panels. Bottom panel: Western blot analysis of caspase-8 and -3 activation showing significant decrease of the uncleaved forms after treatment with EMILIN2 and Δ4 conditioned media (E2 and Δ4, respectively). Conditioned medium (CM) from mock-transfected cells was used as control and vinculin was used as normalizer of protein loading. (E) Right panels: Immunofluorescence analysis of caspase-8 activation after treating HT1080 cells with Δ4 (Δ4); fibronectin and staurosporin (FN and St) were used as negative and positive controls, respectively. Left panels: Nuclei were stained with Hoechst stain. Bar, 20 μm. (F) Left panel: ELISA-based TUNEL assay performed on HT1080 cells transfected with a dominant-negative DR4 or with empty vector (tDR4 or mock, respectively) and challenged with Δ4. Right panel: Schematic representation of the DR4 deletion mutant. *$P \leq .03$.

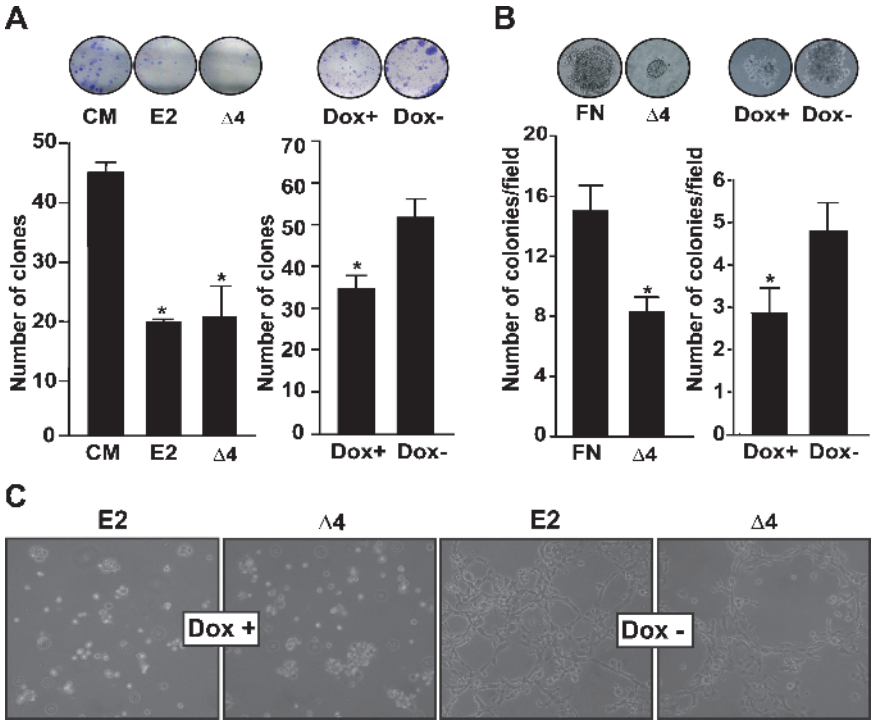

Figure 4. The Δ4 deletion mutant exerts an antitumoral effect *in vitro*. (A) Clonogenic assay performed on HT1080 cells treated with mock, EMILIN2, or Δ4 conditioned media (CM, E2, and Δ4, respectively; left panel) or after transduction with the Δ4 adenoviral vector, with or without doxycycline (Dox+ and Dox−, respectively; right panel). Top panel: Representative pictures. (B) Soft agar colony assay performed on HT1080 cells challenged with Δ4 or fibronectin (Δ4 and FN, respectively; left panel) or after transduction with the Δ4 adenoviral vector, with or without doxycycline (Dox+ and Dox−, respectively; right panel). Top panel: Representative pictures. (C) Matrigel-included HT1080 cells transduced with the EMILIN2 or Δ4 adenoviral constructs (E2 and Δ4, respectively) with or without doxycycline (Dox+ and Dox−, respectively). Bar, 75 μm; $*P \leq .05$.

Alternatively, two groups of four animals were subcutaneously injected with 1×10^6 EMILIN2- or EMILIN2-Δ4–transduced HT1080 cells in the right flank and with Tet-On–transduced cells, used as a control, in the left flank. The cell number was carefully evaluated by vital dye exclusion (Trypan blue; Invitrogen S.r.l.); thus, a comparable number of vital cells were injected in the different groups of animals. Drinkable water was added with 1 mg/ml doxycycline and 2.5% sucrose, given to the animals 2 days before tumor injection and changed every 2 days. In other experiments, 500 μg of bevacizumab per mouse (Roche Pharma AG, Germany) was intraperitoneally injected 2 days after cell injection.

Five other BALB/c nude mice were subcutaneously injected with 1×10^6 HT1080 cells and treated with 20 μg of purified EMILIN2 or Δ4 mutant or PBS at days 2, 5, and 9 after the implant.

Software and Instruments and Data Analysis

The graphs and statistical analysis were generated using Microsoft Office Excel (Microsoft Italia, Segrate, Italy) and SigmaPlot software (Systat Software Inc., San Jose, CA). Densitometric analysis was performed using the Image Tool Software. Cell count and analysis of viability were performed with Countess Automated Cell Counter and the relative software (Invitrogen S.r.l.). *In vivo* imaging acquisitions were performed using the IVIS Imaging System 100 Series (Caliper Life Sciences). Evaluation of the light units for the luminescent substrates was carried out with a luminometer (PerkinElmer, Inc., Waltham, MA). Data analysis was performed using Living Image 3.0 software (Caliper Life Sciences). All images have been assembled using Adobe Illustrator CS and Adobe Photoshop CS (Adobe Systems Inc., San Jose, CA).

Results

Localization of the Proapoptotic Region of EMILIN2

To investigate the proapoptotic effects of EMILIN2 in detail, we have generated an inducible adenoviral construct. This system allowed an efficient expression of the molecule, which can be turned on by the addition of doxycycline and is particularly suitable for both *in vitro* and *in vivo* studies (Figure 1*A*). As expected from our previous observations [32], this approach overexpressing EMILIN2 also led to a significant decrease in tumor cell viability, which correlated with a dramatic increase in the cell death rate. This effect is distinctive of EMILIN2 because treatment with other members of the family such as EMILIN1 or Multimerin2 did not affect tumor cell viability (Figure 1*B*). Moreover, only cancer cells were susceptible to the EMILIN2-driven proapoptotic activity (Figure 1*C*). Transduction of normal dermal fibroblasts, among other normal cells (data not shown), with the EMILIN2 adenoviral vector did not affect their viability as detected by the MTT assay, confirming the results obtained with another cell model [32] (Figure 1*D*). To determine which region of the molecule was responsible for these effects, we have generated a series of deletion mutants (Figure 2, *A* and *B*). In this case, the purified recombinant molecules were used to challenge HT1080 cells. As shown in Figure 2*C*, the Δ1 and the Δ2 deletion mutants

did not affect cell viability, whereas the Δ3 and the Δ4 were as effective as the whole molecule. Because the Δ4 fragment was the smallest deletion retaining the proapoptotic activity, we have chosen this portion for most of the subsequent analysis. This recombinant fragment is soluble and likely preserves a proper three-dimensional structure because it self-assembled *in vitro* to form homotrimers, as demonstrated by native PAGE analysis (Figure W1). The treatment of HT1080 cells with Δ4 led to a dramatic increase in their apoptotic rate, comparable to that induced by the whole molecule or by TRAIL (Figure 2*D*). This effect was also evident after transduction of HT1080 cells with the Δ4 adenoviral construct (Figure 3, *A* and *B*). The mechanism of action activated by the fragment recapitulates that of the whole molecule described in our previous study [32]. This fragment in fact binds to death receptor DR4 (Figure 3, *C* and *D*), leading to receptor activation, as demonstrated by the induction of DISC assembly followed by caspase-8 cleavage (Figure 3, *D* and *E*). The proapoptotic effect induced by Δ4 was abrogated by overexpressing in HT1080 cells a dominant-negative DR4 mutant lacking the cytoplasmic domain; thus, this function requires an intact receptor (Figure 3*F*).

In Vitro *and* In Vivo *Antitumor Effects of EMILIN2 and Δ4*

To determine whether the EMILIN2 and Δ4 proapoptotic effects could lead to a decreased tumor growth *in vitro*, we first set up a clonogenic assay. As shown in Figure 4*A*, HT1080 cells challenged with EMILIN2 or Δ4 formed 50% less colonies in comparison with the control. Similar results were obtained with the use of the Δ4 adenoviral vector (Figure 4*A*, *right panel*). The Δ4 fragment also halted the number of colonies developed in soft agar either using the recombinant molecule or after transduction with the recombinant adenovirus (Figure 4*B*). Moreover, Δ4 impaired the growth of tumor cells in a three-dimensional context, despite the prosurvival stimuli provided by the growth factors and ECM Matrigel components (Figure 4*C*), as previously demonstrated for the entire molecule [32]. Next, to verify whether EMILIN2 could also decrease tumor growth *in vivo*, EGFP-expressing HT1080 cells were injected in nude mice, and the tumor masses were then challenged with purified recombinant EMILIN2. The treatment led to a significant decrease of tumor growth (Figure 5*A*). Analogous results were obtained, challenging established tumors with recombinant EMILIN2 (Figure W2). Accordingly, overexpression of EMILIN2 after transduction with the adenoviral vector led to a remarkable inhibition of tumor growth (Figure 5*B*). Similar results were obtained treating the tumors with recombinant Δ3 (Figure 5*C*) or transducing the cells with the Δ4 adenoviral vector (Figure 5*D*).

Complete Regression of Tumor Growth after Treatment with Δ4 in Combination with Bevacizumab

TUNEL assay analysis performed on the tumor sections revealed that the tumors treated with EMILIN2 or Δ4 displayed a significant increase in tumor cell apoptosis compared with the controls (Figure 6*A*). The augmented intratumoral apoptosis was prompted by the activation of extrinsic pathway initiator caspase-8, which in turn

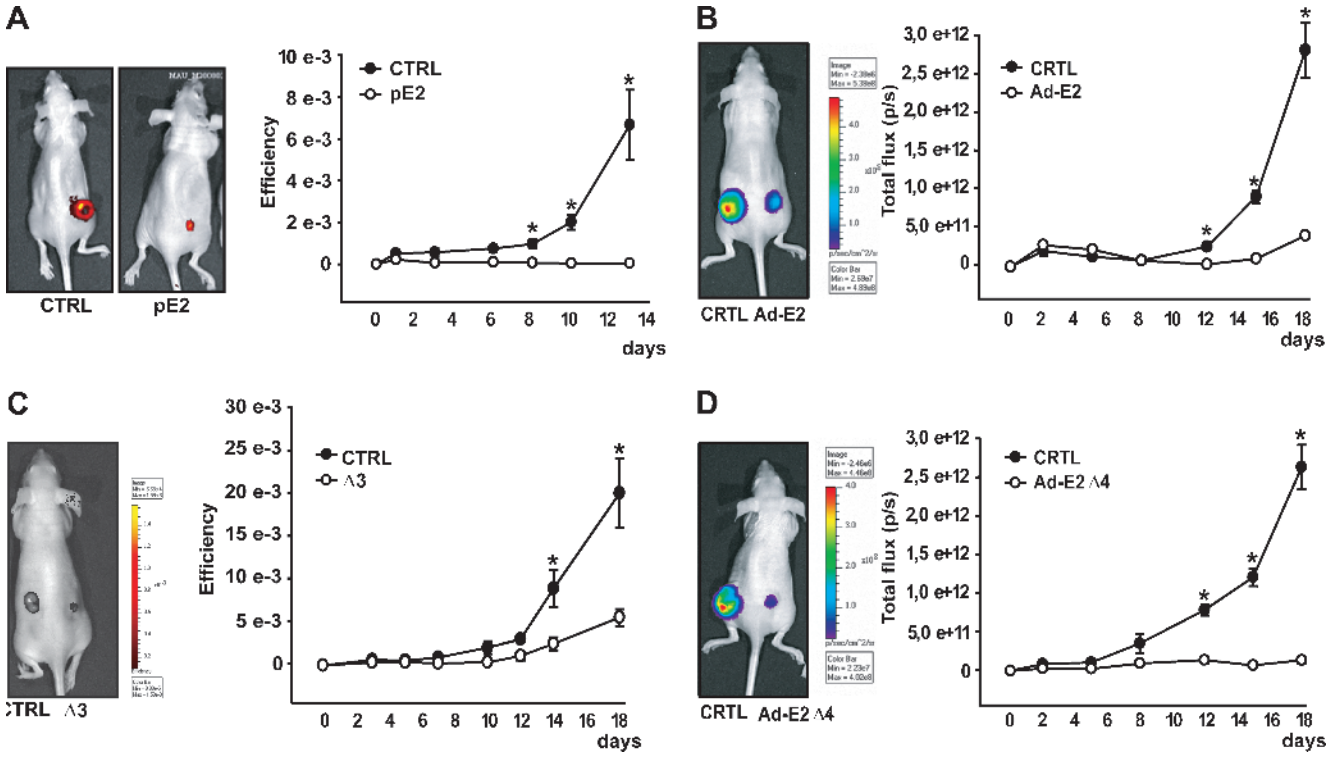

Figure 5. The Δ4 deletion mutant affects tumor growth *in vivo*. (A) *In vivo* imaging analysis of fluorescently labeled HT1080 tumors treated every other day with PBS or recombinant EMILIN2 (CTRL or pE2, respectively). (B) *In vivo* imaging analysis of luminescent HT1080 cells transduced with control (CTRL) or EMILIN2 (Ad-E2) adenoviral constructs and injected in the left or right flank of nude mice, respectively. (C) *In vivo* imaging analysis of fluorescently labeled HT1080 tumors treated every other day with PBS or recombinant Δ3 (CTRL or Δ3, respectively). (D) *In vivo* imaging analysis of luminescent HT1080 cells transduced with control adenoviral vector (CRTL) or Δ4 construct (Ad-E2 Δ4) and injected in the left and right flank of nude mice, respectively. *$P \leq .04$.

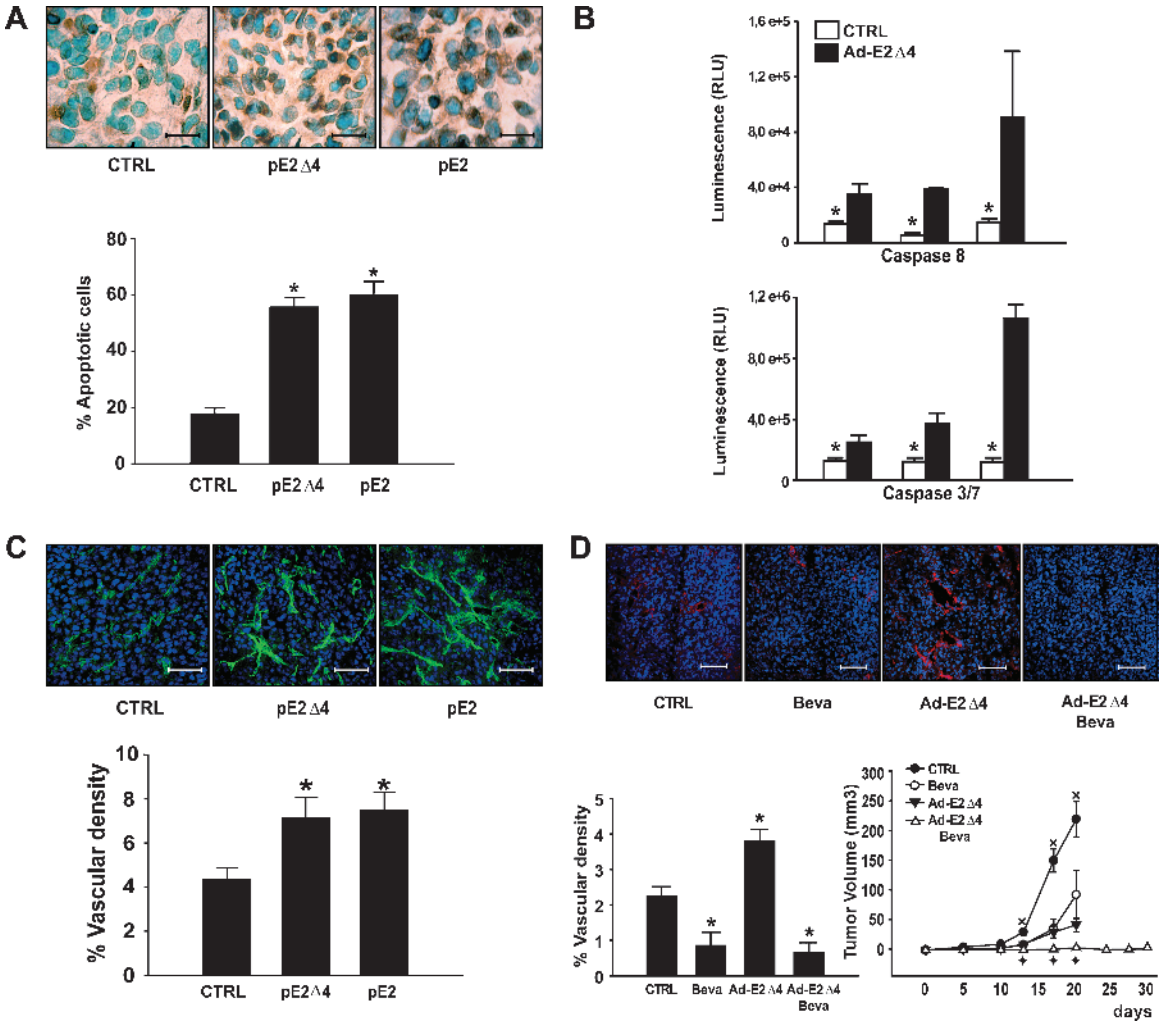

Figure 6. The EMILIN2 antitumoral effects hinge on its proapoptotic effects and are enhanced by antiangiogenic combined therapy. (A) Top panels: Representative pictures of the TUNEL assay performed on sections from tumors treated with PBS, EMILIN2, or Δ4. Bottom graph: Evaluation of tumor cell apoptotic rate. Bar, 20 μm. (B) Caspase-8 and caspase-3/7 activity in tumors from HT1080 cells transduced with the EMILIN2 or Δ4 constructs or empty vector (Ad-E2, Δ4 and CTRL, respectively), as detected by the caspase-Glo assays (top and bottom panels, respectively). Three random tumor samples were chosen. (C) Top panels: Tumor blood vessels immunostaining after treatment with PBS, purified EMILIN2, or Δ4 (CTRL, pE2Δ4, and pE2, respectively). Bottom graph: Evaluation of the vessel density on 10 independent fields was performed with the Image Tool Software. Bar, 75 μm. (D) Tumor blood vessels immunostaining treatment with bevacizumab, Δ4, or Δ4 plus bevacizumab (CTRL, BEVA, pE2Δ4, and pE2Δ4 + BEVA, respectively). Left bottom graph: Evaluation of the vessel density. Bottom right graph: Tumor volume evaluation after injection of HT1080 cells and treatment with PBS, bevacizumab, Δ4, or Δ4 plus bevacizumab (CTRL, BEVA, pE2Δ4, and pE2Δ4 + BEVA, respectively). Bar, 75 μm. The values represent the mean ± SE of 10 tumors per point. $^{*}P \leq .04$, $^{\times}P \leq .03$, between control and treated tumors; ✦ $P \leq .02$, between bevacizumab only and bevacizumab plus Δ4.

activates the effector caspase-3/7 likely accounting for the decreased tumor growth (Figure 6*B*). A more accurate analysis of the tumor sections highlighted the presence of an increased tumor vessels density in the tumors treated with EMILIN2 or Δ4 (Figure 6*C*). This finding prompted us to investigate the efficacy of EMILIN2 and Δ4 in halting tumor growth in combination with the antiangiogenetic antibody bevacizumab. The combination of Δ4 with bevacizumab was strikingly more effective than either treatment alone (Figure 6*D*). In most cases, a total regression of the tumors was observed, and the tumors failed to resume growth even after the withdrawal of bevacizumab treatment and of doxycycline. Only two of the treated tumors formed small masses of approximately 2 mm^3 thus allowing the excision for further analysis. As shown in Figure 6*D*, treatment with bevacizumab was highly effective in reducing the Δ4-dependent vessel density. The depletion of the blood vessels might likely account for the remarkable results obtained with the combined treatment.

EMILIN2 and Δ4 Affect EC Function

The finding that tumors treated with EMILIN2 and Δ4 displayed increased vascularization prompted us to investigate whether EMILIN2 could affect EC function. Whereas treatment with EMILIN2 or Δ4 failed to alter tubules formation in Matrigel (Figure 7*A*), they significantly increased their proliferation rate (Figure 7*B*). In addition, EMILIN2 was found to positively affect EC migration both in tests performed in transwells (Figure 7*B*) and in scratch tests (Figure 7, *C* and *D*). Thus, the increased EC proliferation and migration induced

by EMILIN2 may likely account for the proangiogenic effects observed *in vivo* (Figure 6*C*). Taken together, these results unveil the possibility to develop new promising tools for cancer treatment.

Discussion

In this study, we demonstrate a dual role for EMILIN2. First, we identify that the proapoptotic property resides in a region toward the N-terminus of the molecule: the Δ4 deletion mutant encompasses the features of the entire molecule. It binds to the DR4 receptor, inducing DISC assembly and consequent activation of the extrinsic apoptotic pathway, and it displays a significant antitumorigenic activity *in vitro*. It is interesting to note that in analogy with TRAIL, this fragment is homotrimeric. It is thus conceivable that it might engage death receptors mimicking TRAIL three-dimensional homotrimeric structure rather than the amino acid composition because the two molecules have no sequence homology. In addition, in this study, for the first time, we have analyzed the activity of EMILIN2 and Δ4 *in vivo*. The adenoviral system resulted particularly useful for these studies, especially those involving combinatorial treatments because it prevented the requirement of multiple injections. Our results indicate that tumor growth was significantly impaired by EMILIN2 or Δ4 either over-expressing the molecules or after treatment with the purified proteins. It is interesting to remark that, as shown in Figure 5*B*, the growth of Ad E2 cells in the first 6 days after the injection was comparable to that of the control cells. This indicates that the exogenous EMILIN2, which is removed after the trypsinization and washing procedures, must be resynthesized *in vivo* before exerting its proapoptotic effects. The growth impairment of the tumors challenged with Δ4 correlates with a significant increased activation of the extrinsic apoptotic pathway because activated caspase-8 and caspase-3/7 were enhanced in these samples. Taken together, these observations indicate that the EMILIN2 antitumoral properties can be primarily ascribed to its proapoptotic effects. It is interesting to point out that the proapoptotic activity exerted by this molecule was specific for tumor cells while leaving normal cells unharmed. In fact, the ectopic expression of EMILIN2 or Δ4 in normal skin fibroblasts did not lead to any change in their viability. This aspect is particularly advantageous when dealing with a putative antineoplastic molecule such as the case of TRAIL, which, for its specificity in killing tumor cells, has been proposed as a promising therapeutical tool for the cure of cancer. In fact, several preclinical studies pinpoint the successes encountered with the use of this molecule [18,34–36]. In this context, the EMILIN2 Δ4 region may also represent

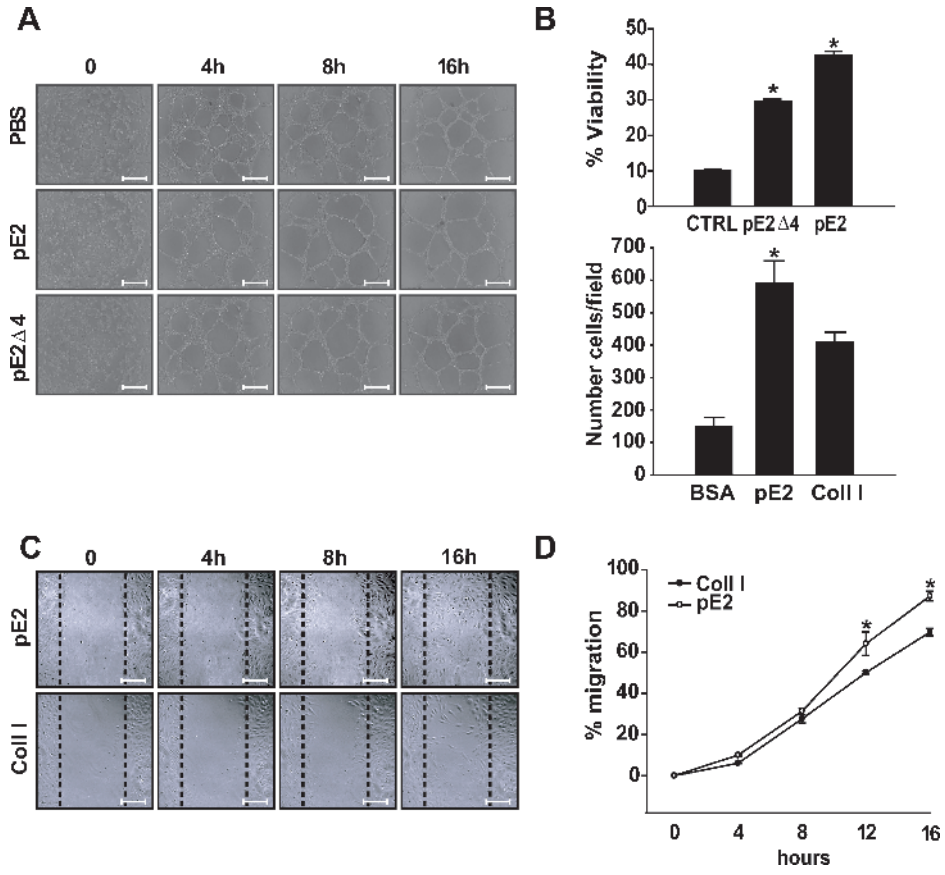

Figure 7. EMILIN2 affects EC proliferation and migration. (A) Pictures taken at four time intervals during *in vitro* tubulogenesis on Matrigel after treatment with 2.5 μg/ml of recombinant EMILIN2 or Δ4; PBS was used as a control (pE2, pE2Δ4, and PBS, respectively). Bar, 75 μm. (B) Top graph: MTT assay performed on HUVECs treated with PBS, Δ4, or EMILIN2 (CTRL, pE2Δ4, and pE2, respectively). Bottom graph: Number of HUVEC migrated cells after transwell membrane coating with 10 μg/ml of denatured BSA, recombinant EMILIN2, or type I collagen (BSA, pE2, and Coll I, respectively). Cells were counted in 10 fields each. (C) Scratch test performed on HUVECs treated with 10 μg/ml of recombinant EMILIN2 or type I collagen (pE2 and Coll I, respectively). Pictures were obtained at different time intervals. Bar, 75 μm. (D) The percentage of cell migration was extrapolated by measuring the area of the scratch covered by the migrating cells by means of the Image Tool Software. Results represent the mean ± SD of three independent experiments. *$P \leq .04$.

a promising approach for the development of novel nontoxic therapeutic tools. EMILIN2 is expressed by a variety of tissues during development, and its deposition decreases in adulthood [37]. It was demonstrated to be expressed in Ewing sarcomas and to be induced by epidermal growth factor and insulin-like growth factor 1 [32]. However, the low or negative expression of EMILIN2 in some tumors should not preclude its usefulness as a potential therapeutic agent. Whether the higher expression of EMILIN2 in some tumor types directly relates to their growth rate is a matter of further investigation provided that appropriate antibody reagents become available.

The second aspect of our findings was that the treatment with EMILIN2 and Δ4, despite the robust reduction of tumor growth, led to a significant increase in the blood vessel density, as observed after a deeper analysis of the cancer lesions. This discovery was supported by *in vitro* experiments where EMILIN2 and Δ4 significantly increased EC proliferation and motility, which likely led to the increased tumor vascularization. Interestingly, the increase in motility is specifically induced on EC only because preliminary data demonstrate that EMILIN2 impinges cell migration of different tumor cell lines (data not shown). The molecular mechanisms, based on the increased EC proliferation and motility induced by EMILIN2, were not investigated here. The $\alpha_4\beta_1$ integrin is a receptor for ECM molecules such as fibronectin and EMILIN1 [38–40]. One possibility would be that it may also function as a receptor for EMILIN2: this integrin is also expressed by ECs [41], and similar to EMILIN1, EMILIN2 bares an inserted sequence in the C1q domain that contains amino acid residues compatible with an $\alpha_4\beta_1$ binding site [42]. Thus, the proangiogenic activity of EMILIN2 might be related to integrin ligation. However, this possibility seems unlikely because the Δ4 mutant is as effective as the whole EMILIN2 molecule in inducing angiogenesis. Alternatively, EMILIN2 and Δ4 might engage a still unknown cell surface receptor. Finally, EMILIN2 and Δ4 may function as a reservoir for cytokines that activate specific receptor tyrosine kinases at the EC surface driving in turn the angiogenic response. The combined treatment with EMILIN2 or Δ4 and bevacizumab [43,44] successfully improved the cure rate and, in most cases, led to the complete regression of the tumors. These results indicate that the residual tumor growth observed after the treatment with EMILIN2 or Δ4 was sustained by increased tumor perfusion. It is known that VEGF, which is recognized to display antiapoptotic effects [45], as well as its receptor, is expressed by tumor cells thus establishing a positive loop of stimulation. By removing a key prosurvival stimulus, the blockage of VEGF with bevacizumab may shift the balance toward the proapoptotic action of EMILIN2 and Δ4. In addition, increased blood vessel perfusion prompted by EMILIN2/Δ4 may favor drug delivery, leading to a paradoxical higher efficiency in blocking tumor vessel formation by antiangiogenic or conventional cytotoxic drugs. Conversely, normalization of tumor vasculature induced by antiangiogenic therapy [46] may enhance Δ4 delivery within the tumor thus allowing a more effective proapoptotic therapy.

In conclusion, there are at least three aspects that render the cotreatment with EMILIN2 and bevacizumab particularly promising. First, both molecules do not harm normal cells. Second, bevacizumab, despite the fact that it enhances tumor hypoxia, abolishes the undesired increase in blood vessel formation induced by EMILIN2, simultaneously sensitizing the cells to the EMILIN2 proapoptotic action, thus improving the efficacy of the treatments [47]. Third, the initial increased tumor perfusion induced by EMILIN2, as well as the vasculature normalization induced by bevacizumab, may facilitate drug delivery. Taken together, these results highlight a potent antitumoral effect *in vivo* of a 90-residue long EMILIN2 region. Owing to the lack of cytotoxicity for normal cells, it is conceivable that this molecule or specific peptide encompassing the proapoptotic deletion mutant might be applied in the future as an antitumoral agent especially in combination with antiangiogenic drugs such as bevacizumab.

References

[1] Kalluri R and Zeisberg M (2006). Fibroblasts in cancer. *Nat Rev Cancer* **6**, 392–401.

[2] Sund M and Kalluri R (2009). Tumor stroma derived biomarkers in cancer. *Cancer Metastasis Rev* **28**, 177–183.

[3] Geiger TR and Peeper DS (2009). Metastasis mechanisms. *Biochim Biophys Acta* **1796**, 293–308.

[4] Folkman J (1971). Tumor angiogenesis: therapeutic implications. *N Engl J Med* **285**, 1182–1186.

[5] Thompson Coon JS, Liu Z, Hoyle M, Rogers G, Green C, Moxham T, Welch K, and Stein K (2009). Sunitinib and bevacizumab for first-line treatment of metastatic renal cell carcinoma: a systematic review and indirect comparison of clinical effectiveness. *Br J Cancer* **101**, 238–243.

[6] Sharieff W (2004). Bevacizumab in colorectal cancer. *N Engl J Med* **351**, 1690–1691.

[7] Sirohi B and Smith K (2008). Bevacizumab in the treatment of breast cancer. *Expert Rev Anticancer Ther* **8**, 1559–1568.

[8] Tol J, Koopman M, Cats A, Rodenburg CJ, Creemers GJ, Schrama JG, Erdkamp FL, Vos AH, van Groeningen CJ, Sinnige HA, et al. (2009). Chemotherapy, bevacizumab, and cetuximab in metastatic colorectal cancer. *N Engl J Med* **360**, 563–572.

[9] Tao X, Sood AK, Deavers MT, Schmeler KM, Nick AM, Coleman RL, Milojevic L, Gershenson DM, and Brown J (2009). Anti-angiogenesis therapy with bevacizumab for patients with ovarian granulosa cell tumors. *Gynecol Oncol* **114**, 431–436.

[10] Hanahan D and Weinberg RA (2000). The hallmarks of cancer. *Cell* **100**, 57–70.

[11] Fulda S (2009). Tumor resistance to apoptosis. *Int J Cancer* **124**, 511–515.

[12] Hengartner MO (2000). The biochemistry of apoptosis. *Nature* **407**, 770–776.

[13] Pan G, O'Rourke K, Chinnaiyan AM, Gentz R, Ebner R, Ni J, and Dixit VM (1997). The receptor for the cytotoxic ligand TRAIL. *Science* **276**, 111–113.

[14] Walczak H, gli-Esposti MA, Johnson RS, Smolak PJ, Waugh JY, Boiani N, Timour MS, Gerhart MJ, Schooley KA, Smith CA, et al. (1997). TRAIL-R2: a novel apoptosis-mediating receptor for TRAIL. *EMBO J* **16**, 5386–5397.

[15] LeBlanc HN and Ashkenazi A (2003). Apo2L/TRAIL and its death and decoy receptors. *Cell Death Differ* **10**, 66–75.

[16] Wu CH, Kao CH, and Safa AR (2008). TRAIL recombinant adenovirus triggers robust apoptosis in multidrug-resistant HL-60/Vinc cells preferentially through death receptor DR5. *Hum Gene Ther* **19**, 731–743.

[17] Ashkenazi A (2008). Targeting the extrinsic apoptosis pathway in cancer. *Cytokine Growth Factor Rev* **19**, 325–331.

[18] Johnstone RW, Frew AJ, and Smyth MJ (2008). The TRAIL apoptotic pathway in cancer onset, progression and therapy. *Nat Rev Cancer* **8**, 782–798.

[19] Sprick MR, Weigand MA, Rieser E, Rauch CT, Juo P, Blenis J, Krammer PH, and Walczak H (2000). FADD/MORT1 and caspase-8 are recruited to TRAIL receptors 1 and 2 and are essential for apoptosis mediated by TRAIL receptor 2. *Immunity* **12**, 599–609.

[20] Wang J, Chun HJ, Wong W, Spencer DM, and Lenardo MJ (2001). Caspase-10 is an initiator caspase in death receptor signaling. *Proc Natl Acad Sci USA* **98**, 13884–13888.

[21] Marastoni S, Ligresti G, Lorenzon E, Colombatti A, and Mongiat M (2008). Extracellular matrix: a matter of life and death. *Connect Tissue Res* **49**, 203–206.

[22] Chen Y and Du XY (2007). Functional properties and intracellular signaling of CCN1/Cyr61. *J Cell Biochem* **100**, 1337–1345.

[23] Juric V, Chen CC, and Lau LF (2009). Fas-mediated apoptosis is regulated by the extracellular matrix protein CCN1 (CYR61) *in vitro* and *in vivo*. *Mol Cell Biol* **29**, 3266–3279.

[24] Jimenez B, Volpert OV, Crawford SE, Febbraio M, Silverstein RL, and Bouck N (2000). Signals leading to apoptosis-dependent inhibition of neovascularization by thrombospondin-1. *Nat Med* **6**, 41–48.

[25] Shichiri M and Hirata Y (2001). Antiangiogenesis signals by endostatin. *FASEB J* **15**, 1044–1053.

[26] Ramakrishnan S, Nguyen TM, Subramanian IV, and Kelekar A (2007). Autophagy and angiogenesis inhibition. *Autophagy* **3**, 512–515.
[27] Tai IT and Tang MJ (2008). SPARC in cancer biology: its role in cancer progression and potential for therapy. *Drug Resist Updat* **11**, 231–246.
[28] Tang MJ and Tai IT (2007). A novel interaction between procaspase 8 and SPARC enhances apoptosis and potentiates chemotherapy sensitivity in colorectal cancers. *J Biol Chem* **282**, 34457–34467.
[29] Seidler DG, Goldoni S, Agnew C, Cardi C, Thakur ML, Owens RT, McQuillan DJ, and Iozzo RV (2006). Decorin protein core inhibits *in vivo* cancer growth and metabolism by hindering epidermal growth factor receptor function and triggering apoptosis via caspase-3 activation. *J Biol Chem* **281**, 26408–26418.
[30] Doliana R, Bot S, Bonaldo P, and Colombatti A (2000). EMI, a novel cysteine-rich domain of EMILINs and other extracellular proteins, interacts with the gC1q domains and participates in multimerization. *FEBS Lett* **484**, 164–168.
[31] Doliana R, Bot S, Mungiguerra G, Canton A, Cilli SP, and Colombatti A (2001). Isolation and characterization of EMILIN-2, a new component of the growing EMILINs family and a member of the EMI domain-containing superfamily. *J Biol Chem* **276**, 12003–12011.
[32] Mongiat M, Ligresti G, Marastoni S, Lorenzon E, Doliana R, and Colombatti A (2007). Regulation of the extrinsic apoptotic pathway by the extracellular matrix glycoprotein EMILIN2. *Mol Cell Biol* **27**, 7176–7187.
[33] Danussi C, Spessotto P, Petrucco A, Wassermann B, Sabatelli P, Montesi M, Doliana R, Bressan GM, and Colombatti A (2008). Emilin1 deficiency causes structural and functional defects of lymphatic vasculature. *Mol Cell Biol* **28**, 4026–4039.
[34] Wang S (2008). The promise of cancer therapeutics targeting the TNF-related apoptosis-inducing ligand and TRAIL receptor pathway. *Oncogene* **27**, 6207–6215.
[35] Ashkenazi A, Holland P, and Eckhardt SG (2008). Ligand-based targeting of apoptosis in cancer: the potential of recombinant human apoptosis ligand 2/tumor necrosis factor–related apoptosis-inducing ligand (rhApo2L/TRAIL). *J Clin Oncol* **26**, 3621–3630.
[36] Duiker EW, Mom CH, de Jong S, Willemse PH, Gietema JA, van der Zee AG, and de Vries EG (2006). The clinical trail of TRAIL. *Eur J Cancer* **42**, 2233–2240.
[37] Braghetta P, Ferrari A, De GP, Zanetti M, Volpin D, Bonaldo P, and Bressan GM (2004). Overlapping, complementary and site-specific expression pattern of genes of the EMILIN/Multimerin family. *Matrix Biol* **22**, 549–556.
[38] Williams DA, Rios M, Stephens C, and Patel VP (1991). Fibronectin and VLA-4 in haematopoietic stem cell–microenvironment interactions. *Nature* **352**, 438–441.
[39] Spessotto P, Cervi M, Mucignat MT, Mungiguerra G, Sartoretto I, Doliana R, and Colombatti A (2003). β_1 Integrin–dependent cell adhesion to EMILIN-1 is mediated by the gC1q domain. *J Biol Chem* **278**, 6160–6167.
[40] Spessotto P, Bulla R, Danussi C, Radillo O, Cervi M, Monami G, Bossi F, Tedesco F, Doliana R, and Colombatti A (2006). EMILIN1 represents a major stromal element determining human trophoblast invasion of the uterine wall. *J Cell Sci* **119**, 4574–4584.
[41] Nakao S, Kuwano T, Ishibashi T, Kuwano M, and Ono M (2003). Synergistic effect of TNF-alpha in soluble VCAM-1–induced angiogenesis through alpha 4 integrins. *J Immunol* **170**, 5704–5711.
[42] Verdone G, Doliana R, Corazza A, Colebrooke SA, Spessotto P, Bot S, Bucciotti F, Capuano A, Silvestri A, Viglino P, et al. (2008). The solution structure of EMILIN1 globular C1q domain reveals a disordered insertion necessary for interaction with the $\alpha_4\beta_1$ integrin. *J Biol Chem* **283**, 18947–18956.
[43] Gerber HP and Ferrara N (2005). Pharmacology and pharmacodynamics of bevacizumab as monotherapy or in combination with cytotoxic therapy in preclinical studies. *Cancer Res* **65**, 671–680.
[44] Ferrara N, Hillan KJ, Gerber HP, and Novotny W (2004). Discovery and development of bevacizumab, an anti-VEGF antibody for treating cancer. *Nat Rev Drug Discov* **3**, 391–400.
[45] Epstein RJ (2007). VEGF signaling inhibitors: more pro-apoptotic than anti-angiogenic. *Cancer Metastasis Rev* **26**, 443–452.
[46] Jain RK (2005). Normalization of tumor vasculature: an emerging concept in antiangiogenic therapy. *Science* **307**, 58–62.
[47] Kerbel RS (2006). Antiangiogenic therapy: a universal chemosensitization strategy for cancer? *Science* **312**, 1171–1175.

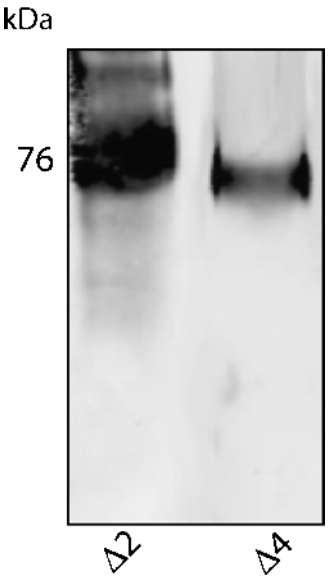

Figure W1. Native polyacrylamide gel analysis of EMILIN2 deletion mutants Δ2 and Δ4. Because biologically active TRAIL is known to form a homotrimer in solution [1], we investigated whether the Δ4 (M_W ~ 26 kDa) could also form homotrimers in solution. We have thus analyzed the protein molecular weight in polyacrylamide gels under native conditions. Besides the α-lactalbumin, carbonic anhydrase, chicken egg albumin, and bovine serum albumin used as standards, we have used the Δ2 (M_W ~ 27 kDa) deletion mutant as a reference for motility because it contains a gC1q domain that behaves as a trimer, as shown for the EMILIN1 gC1q domain [2]. After separation, the proteins were analyzed by Western blot using the α-Penta-His mAb (QIAGEN). On native gels, the two polypeptides displayed a similar migration pattern, also suggesting that the Δ4 deletion mutant forms trimers under native conditions. Because the Asp 206 to Leu 295 (Δ4) region retains the ability to trimerize, it is conceivable that EMILIN2 acts in a similar fashion as the homotrimer of TRAIL, which binds to three death receptor molecules [3], leading to their activation.

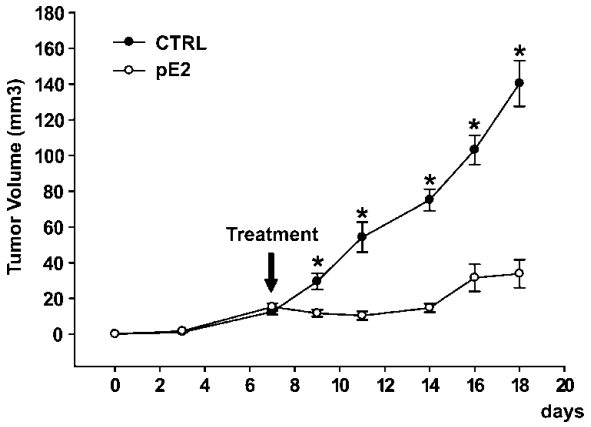

Figure W2. Analysis of EMILIN2 treatment on established tumors. To analyze the effect of EMILIN2 on established tumors, 20 nude mice were injected in the right flank with 1 million HT1080 cells. Once the tumors reached the volume of approximately 15 to 20 mm^3, half of the mice were injected daily intratumorally with 10 μg of EMILIN2 (E2). Control mice were treated with an equal volume of PBS (PBS). The arrow indicates the day when the treatment was started. The values in the graph represent the mean ± SE of the various tumor volumes measured with the caliper using the following formula: $\pi LW^2/6$, where L indicates length and W indicates width. $^*P \leq .005$.

Supplementary References

[1] Cha SS, Kim MS, Choi YH, Sung BJ, Shin NK, Shin HC, Sung YC, and Oh BH (1999). 2.8 A resolution crystal structure of human TRAIL, a cytokine with selective antitumor activity. *Immunity* **11**, 253–261.

[2] Mongiat M, Mungiguerra G, Bot S, Mucignat MT, Giacomello E, Doliana R, and Colombatti A (2000). Self-assembly and supramolecular organization of EMILIN. *J Biol Chem* **275**, 25471–25480.

[3] Mongkolsapaya J, Grimes JM, Chen N, Xu XN, Stuart DI, Jones EY, and Screaton GR (1999). Structure of the TRAIL-DR5 complex reveals mechanisms conferring specificity in apoptotic initiation. *Nat Struct Biol* **6**, 1048–1053.